Journal of Radiotherapy in Practice

Journal of Radiotherapy in Practice (2017)
16, 183–198 © Cambridge University Press 2017
doi:10.1017/S1460396916000601

Original Article

Radiation-induced biological changes of neural structures in the base of the skull tumours

C. Gh. Buzea[1], C. Mirestean[1], Irina Butuc[1], A. Zara[1], D. T. Iancu[2]

[1]*Regional Institute of Oncology, Iasi, Romania,* [2] *'Grigore T. Popa', University of Medicine and Pharmacy, Iasi, Romania*

(Received 20 July 2016; revised 7 December 2016; accepted 11 December 2016; first published online 18 January 2017)

Abstract

Background and purpose: The aim of this paper is to compare neural induced changes in three-dimensional conformal radiotherapy (3D-CRT) versus intensity modulated radiation therapy (IMRT) and volumetric modulated arc therapy (VMAT) for nasopharyngeal cancers.

Materials and methods: Radiotherapy plans for 10 patients with nasopharyngeal cancer stages III and IV were prospectively developed for 3D-CRT, IMRT and VMAT using Varian Eclipse planning system. The same radiation therapist carried out all planning and the same clinical dosimetric constraints were used. Normal tissue complication probabilities were calculated.

Results: The mean planning target volume's (PTVs) conformity index (CI) for 3D-CRT was 1·424, for IMRT 1·1, and for VMAT 1·081. The PTV homogeneity (HI) index was 0·204 for 3D-CRT, 0·124 for IMRT and 0·153 for VMAT. Normal tissue complication probabilities gave complex results for 3D-CRT, IMRT and VMAT and are analysed in detail in this paper. The mean monitor units were 95 (range 9–180) for 3D-CRT; 165 (range 52–277) for IMRT; and 331 (range 167–494) for VMAT ($p < 0{\cdot}05$).

Conclusions: VMAT is associated with similar dosimetric advantages as IMRT over 3D-CRT for nasopharyngeal cancer. VMAT is associated with faster delivery times and greater number of mean monitor units than IMRT. Brain radionecrosis severity and risk, in the past, have been underestimated. By improving the life expectancy of patients with nasopharyngeal cancer to ensure maintenance of the neural structures, recommended dose limits should be considered as a first degree priority (as the spinal cord, brainstem, etc.) when IMRT and VMAT plans are implemented.

Keywords: intensity modulated radiation therapy; nasopharyngeal cancer; volumetric modulated arc therapy

INTRODUCTION

Nasopharyngeal cancer is the leading type of cancer in the southeastern region of China with an incidence of up to 25–50/100,000 inhabitants

Correspondence to: C. Gh. Buzea, Regional Institute of Oncology, Henry Mathias Berthelot 2–4, Iasi, Romania Tel: +40 753 675353. Fax: +40 232 231132. E-mail: calinb2003@yahoo.com

while in Europe the incidence is ~1/100,000 population.[1] Due to its anatomical positioning and high radiosensitivity, radiation therapy is the treatment of choice.[2]

Approximately 44% of patients with nasopharyngeal cancer treated with radiation will present late complications including cranial nerves paresis (20%), osteoradionecrosis of skull base (17%) and radionecrosis of temporal lobe (8%). Cerebral radionecrosis, in particular of the temporal lobe is one of the most serious late complication.[3] Five-year survival among patients with temporal lobe necrosis was estimated at about 59%. Intensity modulated radiation therapy (IMRT) technique has reduced xerostomia and trismus but excluding the temporal lobe from the radiation field is impossible both in two-dimensional (2D) and 3D radiotherapy and in inverse planning techniques, due to its medial section location bilaterally near the base of the skull.[2]

Clinical manifestations of the temporal lobe necrosis include: dizziness and memory problems, personality changes, seizures, but also symptoms associated with mass effect and increased intracranial pressure (generalised seizures, moderate headache, confusion).[4]

Although rare, myelopathy is one of the most severe and debilitating complications of head-and-neck cancer radiotherapy. In the era of conventional radiotherapy, a dose of 43–45 Gy in 22–25 fractions was considered the limit of bone marrow tolerance. Although, to protect the cervical spine, blocks of lead were placed in the way of opposite side beams, spine continued to receive a dose of ~6·2 Gy without reporting a high rate of complications.[5] Subsequent studies revealed a complication rate <1% and <10% for a dose of 54 and 61 Gy, respectively, and a dose/fraction dependence.[6]

Implementation of the IMRT technique as standard in radiation therapy of head-and-neck, had as consequence a reduced dose received by the bone marrow, however, non-fatal myelopathies (presence of Lhermitte sign) have been reported, perceived by the patient as an electric shock produced at neck flexion, radiating to extremities.[7] The increased incidence of this syndrome observed after chemo – IMRT with carboplatin – paclitaxel, induced 'medullary tolerance decrease hypothesis' due to both the 'bath and shower' effect (the presence of high doses in the vicinity of low doses) and chemotherapy.[8]

Toxicity through radionecrosis of the brainstem is rare, being reported in about 100 cases in the literature, but given the functional importance of the brainstem and the lethal potential, this is very serious. The data on the effect of small volumes irradiated with high doses is insufficient. A safe dose limit is considered as a maximum dose of 54 Gy in standard fractionation (1·8–2 Gy) and small volumes of 1–10 ml can receive up to 59 Gy. Severe effects have been reported over the dose of 64 Gy, hypo-fractionation being a supplementary risk factor.[9]

Irradiation of the brainstem, particular the area postrema and the dorsal vagal nucleus, was correlated with nausea and vomiting. Studies on patients with nasopharyngeal cancer treated by IMRT technique revealed that one must delineate the dorsal vagal and vestibular nuclei as organs at risk.[10,11]

As a cutting edge treatment for head-and-neck carcinomas has evolved from three-dimensional conformal radiotherapy (3D-CRT) to IMRT, the clinical benefits of reducing dose to the parotid glands have been exhibited[12–15] with resulting decreasing xerostomia for patients treated with IMRT in contrast to 3D-CRT. The fundamental downside of IMRT is the more intricate and time consuming treatment planning process and the requirement for more extensive quality assurance physics. Likewise, IMRT uses a higher number of static beams and monitor units (MUs),[16] which increases the radiation delivery times up to 20 minutes and at the same time, the patient exposure to low-dose irradiation.

Overall, an increase in the number of IMRT beams augments the degrees of freedom,[17] making intensity modulated arc therapy a coherent next step in IMRT delivery. A few optimisation techniques for arc therapy in view of direct aperture optimisation have been depicted.[18–20] The novel methodology for volumetric modulated arc therapy empowers IMRT-like dose distributions to be delivered using a single

https://doi.org/10.1017/S1460396916000601 Published online by Cambridge University Press

rotation of the gantry.[21] Volumetric modulated arc therapy (VMAT) has been clinically implemented in the Eclipse treatment planning software (Varian Medical Systems, Palo Alto, CA, USA) under the name of RapidArc (RA) (which is the same as VMAT). In RA, the gantry speed and dose rate vary in a continuous way during delivery. In addition, there is full leaf interdigitation, permitting multiple little islands of dose to be delivered to the target volume at every gantry position. Clinical presentation of such new treatment procedures must be preceded by detailed validation of a series of plans.[22,23] Broad studies on treatment planning or dosimetric approval and correlation of RA measurements dispersion with those produced by existing IMRT systems have not yet been accounted for. As IMRT plans for head-and-neck cancer are requesting and require solid dose modulation, we chose these tumours for a comparative analysis of RA plans with IMRT and 3D-CRT.

In this paper, we use radiobiological models to assess changes induced by irradiation of nerve structures (i.e. critical organs) in the treatment of the base of the skull tumours. RADBIOMOD, a simple program for utilising biological modelling in radiotherapy plan evaluation was used. It has been developed using Visual Basic for Applications for Microsoft Excel that incorporates multiple different biological models for radiotherapy plan evaluation, including modified Poisson tumour control probability (TCP), modified Zaider–Minerbo TCP, Lyman–Kutcher–Burman normal tissue complication probability (NTCP), equivalent uniform dose (EUD), EUD-based TCP, EUD-based NTCP and uncomplicated TCP.[24]

Consequently, we chose tumours of the nasopharynx (cavum) involving the base of the skull, that have been irradiated by 3D-CRT, IMRT and VMAT techniques for curative purpose in the multimodal combined hormone–radiation therapy treatment. We evaluate the integrity of nerve structures belonging to the cervical–cephalic segment (spinal cord, brainstem, optical chiasm, optical nerves, brain) both in terms of structural integrity, dose coverage and of possible clinical complications. The study was conducted on a total of 10 patients and over a two-year period.

METHODS AND MATERIALS

All of the patients received the treatment with 3D-CRT before IMRT and VMAT techniques were implemented and alternative IMRT and VMAT plans were created. All the treatment plans were constructed in the same computed tomography (CT) and structure set. The median age was 45, with six males and four females. The clinical stage distribution was T3 in six patients and T4 in four patients with node stage N2-N3.

Treatment protocol

Head-and-neck tumours and their treatments can cause complex anatomical and functional deficits. A thorough initial assessment of tumour and patient factors including function, comorbidity and personal preference is essential to choose the optimal treatment pathway. Conformal radiotherapy of head-and-neck cancers requires knowledge of anatomy and patterns of spread of disease, which are often specific to each tumour site.

Patients underwent CT simulation using 3 mm thick slices by 3 mm spacing, from 2 cm above the superior orbital ridge (to include the skull base) to the arch of the aorta inferiorly. Even though intravenous contrast may help definition of cervical nodes, no oral or intravenous contrast was used at simulation. Reference marks were placed on the shell at the CT visit to aid verification. Patients were treated supine with head and shoulders immobilised in a Perspex shell or thermoplastic mask with at least five fixation points.

A single radiation oncologist completed contouring before commencement of the project. The gross tumour volume (GTV) is first contoured on the planning CT using diagnostic images and clinical information. Particular attention is given to the parapharyngeal space, and to the lateral pharyngeal lymph nodes. Retropharyngeal nodes >5 mm and cervical nodes >10 mm in short axis diameter are contoured as GTV. The GTV is expanded isotropically by 5 mm to form the clinical target volume (CTV) 70 which is then edited to reflect natural tumour boundaries. Numbers 50, 66, 70 added to GTV, CTV and planning target volume (PTV)

https://doi.org/10.1017/S1460396916000601 Published online by Cambridge University Press

represent the radiation dose in Gy received by the target volumes corresponding to anatomical structures delineated, used in our department after the implementation of the 3D-CRT technique, based on guideline recommendations.[25]

Three CTVs are defined: a high-dose CTV70 reflecting the clinically apparent disease; a high-risk CTV66 reflecting the high risk of local spread in and adjacent to the nasopharynx; and a prophylactic CTV50 to treat at risk but clinically uninvolved nodes. The CTV70 is copied to form the CTV66 which is expanded to reflect possible local spread in the nasopharynx. The treatment volume includes the whole nasopharynx, adjacent retropharyngeal lymph nodal regions, parapharyngeal space, pterygoid plates, pterygomaxillary fissures, floor of the sphenoid sinus, foramen lacerum and the posterior part of the nasal cavity (5 mm anterior to the GTV).

A CTV-PTV margin is applied (usually 3–5 mm) based on measured set-up errors assuming no tumour motion.

The brain, brainstem and spinal cord were delineated. The parotid glands, cochlea and optic apparatus were also contoured as critical structures as IMRT and VMAT are going to be used and dose sparing may be possible. Also, we mention that parotid glands and cochlea were considered second degree priority OAR's, and the target volume was not compromised to spare them.

All 3D-CRT, IMRT and VMAT plans were created prospectively using the unique set of contours for each patient. A standalone Eclipse treatment planning system, installed on a Dell Precision T5500 computer, was used for all plan creation.

The treatment plans were based on nasopharynx (cavum) treatment with a three-phase treatment. The study was based on the original planning CT and contoured volumes in each of the 10 patients (Figure 1). The CTV's consisted of the GTVs and the critical structures as defined above.

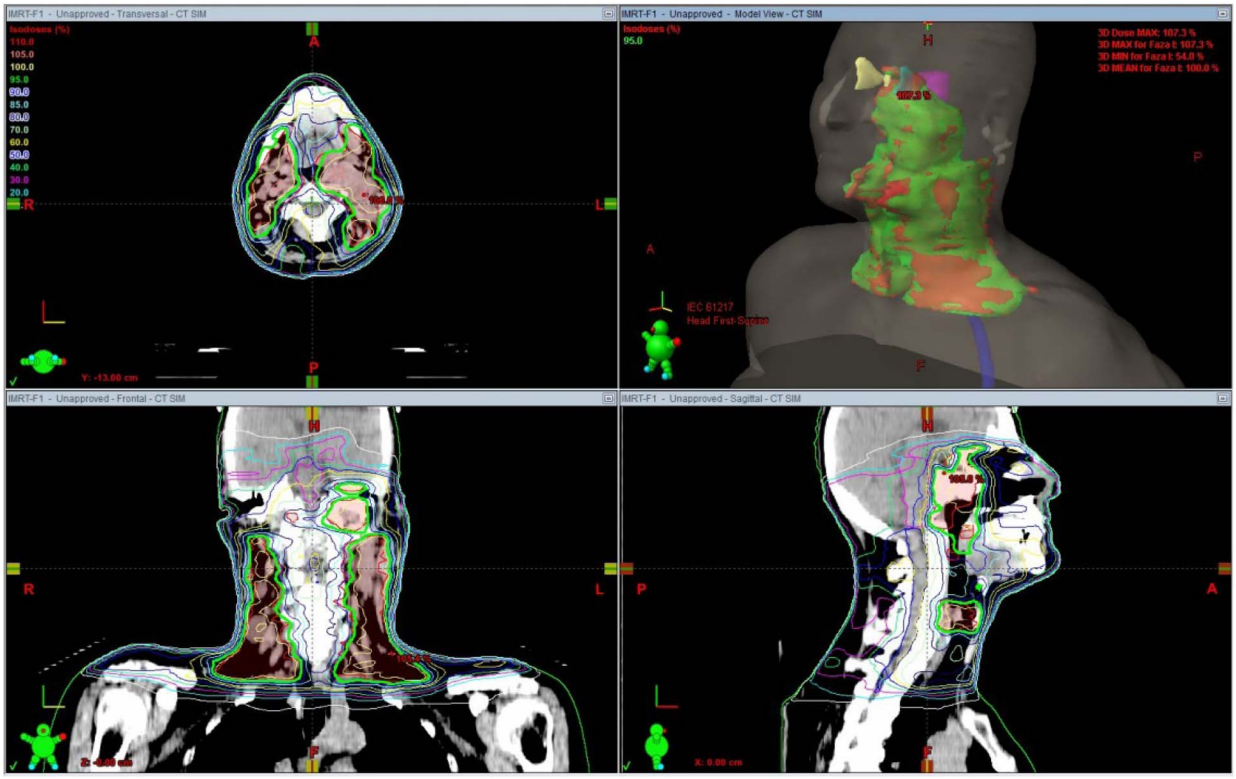

Figure 1. Eclipse treatment plan window for one of the 10 patients.

https://doi.org/10.1017/S1460396916000601 Published online by Cambridge University Press

Table 1. Clinical dosimetric constraints used in planning three-dimensional conformal radiotherapy/intensity modulated radiation therapy/volumetric modulated arc therapy (3D-CRT/IMRT/VMAT)

	Dose to 0·1 cm^3	Dose to <1 cm^3	Mean dose
Spinal cord	46 Gy	45 Gy	
Brainstem	55 Gy	54 Gy	40 Gy
Brain		60 Gy	
Whole parotid			24 Gy – if aiming to preserve function
Mandible		74 Gy	<33% to receive >65 Gy
Larynx			Aim for 50 Gy but do not allow to compromise PTV coverage
Lens			<6–8 Gy
Retina	50 Gy		45 Gy. If greater consent for possible visual loss
Optic chiasm/nerves	54 Gy		Can increase to 55–60 Gy at clinician's discretion/patient's consent
Oral cavity			Aim for 45 Gy
Cornea			Dmax 40 Gy
Lacrimal gland			Dmax 30 Gy

Note: PTV, planning target volume.

Each patient had one 3D-CRT, one IMRT and one VMAT plan created by the same medical physicist. The medical physicist had extensive experience with 3D-CRT, IMRT and VMAT planning. The same dose constraints were used for creation of 3D-CRT, IMRT and VMAT plans (Table 1).

The total prescription dose on the PTV was based on a median dose of 70 Gy delivered in 35 fractions at 2 Gy/fraction treating daily, five days per week over seven weeks, 49 days. It was divided between PTV50 (Phase I): a dose of 50 Gy delivered in 25 fractions at 2 Gy/fraction, PTV66 (Phase II): a dose of 16 Gy delivered in eight fractions at 2 Gy/fraction and PTV70 (Phase III): a dose of 4 Gy delivered in two fractions at 2 Gy/fraction treating daily. Plans were normalised to ensure that the 95% isodose adequately covered the PTV and that the dose distribution was such that the minimum dose to 99% of the PTV (D99%) was ≥95% of the prescribed dose (50, 66 and 70 Gy, respectively) and the mean CTV dose was within 0·5 Gy of the prescribed dose. All plans were evaluated to ensure they met our institutional dose constraints outlined in Table 1. All 3D-CRT plans were composed of an adequate number of beam field arrangements using 6 MV photons. MLC beam shaping, beam modifiers (e.g. wedges) and field-in-field were employed as required to produce the most conformal dosimetry. All IMRT and VMAT plans were created using a 6 MV photon beam applicable to a Varian Clinac iX (Varian Medical Systems) linear accelerator with a 120 leaf Millennium dynamic multileaf collimator (MLC); 6 MV photons were used for IMRT and VMAT as this reflected most published clinical studies as well as current practice in our institution.[26]

IMRT plans

IMRT plans were generated on the Eclipse Version 11.0.31 treatment planning software using a 5–9 beam multi-field technique. The number of beams, and their position were automatically calculated using the built in Beam Angle Optimization 11.0.31 software facility, or were set up manually, according to the complexity of the target volume. The initial optimisation parameters and their priorities were established according to our institutional optimisation protocol and then adjusted as required to achieve the dose constraints (Table 1) using a minimum of 100 iterations. A normal tissue objective was encompassed and the default smoothing parameters were applied to help reduce hotspots outside the target volume and the total number of MUs.

VMAT plans

VMAT plans using the Varian Rapid-Arc technique (Varian Medical Systems) were planned using Eclipse Version 11.0.31 treatment planning software using the same CT-data set and contoured volumes as the IMRT plans. A single arc

https://doi.org/10.1017/S1460396916000601 Published online by Cambridge University Press

technique was used with the gantry set to rotate through 360° in a clockwise direction from a starting position of 181° to a final position of 179°, and a double arc technique with the gantry set to rotate through 360° in a clockwise direction from a starting position of 181° to a final position of 179°, and through 360° in a counterclockwise direction from a starting position of 179° to a final position of 181° according to the complexity of the phase being treated. The collimator rotation was individually optimised for each patient but generally set at 30° and 330° to reduce the effect of tongue and groove leakage.

The final dose calculation for all three of the plans for each of the 10 patients was performed using the anisotropic analytical algorithm version 11.0.31 with a 2·5 mm dose calculation grid space.

Treatment delivery

Treatment delivery for each of the 10 plans (3D-CRT, IMRT and VMAT) employed a Varian 21iX linear accelerator (Varian Medical Systems). All of the beams were delivered to a void bunker for IMRT and VMAT plans.

Conformity and homogeneity

Conformity and homogeneity of the plans was measured by the conformity index (CI) which is a proportion of the volume of tissue getting no <95% (V95) of the prescribed dose divided by

Table 2. *Conformity index (CI) three-dimensional conformal radiotherapy/intensity modulated radiation therapy/volumetric modulated arc therapy (3D-CRT/IMRT/VMAT)*

	3D			IMRT			VMAT			
	F1	F2	F3	F1	F2	F3	F1	F2	F3	
1	723·71	402·41	282·85	635·87	451·47	270·32	582·82	377·73	267	V95
	555·7	356·1	258·6	555·7	356·1	258·6	555·7	356·1	258·6	VPTV
CI	1·302	1·130	1·094	1·144	1·268	1·045	1·049	1·061	1·032	
2	832·18	551	170·82	500·88	295·99	126·55	556·64	343·19	125·88	V95
	448·2	280·2	117·9	448·2	280·2	117·9	448·2	280·2	117·9	VPTV
CI	1·857	1·966	1·449	1·118	1·056	1·073	1·242	1·225	1·068	
3	935·58	642·21	194·85	740·88	501·46	157·4	576·22	435	143·53	V95
	547·7	374·3	132·4	547·7	374·3	132·4	547·7	374·3	132·4	VPTV
CI	1·708	1·716	1·472	1·353	1·340	1·189	1·052	1·162	1·084	
4	725·98	494·49	250·1	518·86	373·25	184·42	514·87	377·35	181·57	V95
	464·9	344·9	165·3	464·9	344·9	165·3	464·9	344·9	165·3	VPTV
CI	1·562	1·434	1·513	1·116	1·082	1·116	1·107	1·094	1·098	
5	631·2	369·63	111·88	379·37	256·81	90·39	423·09	271·02	88·72	V95
	377·2	237·8	83	377·2	237·8	83	377·2	237·8	83	VPTV
CI	1·673	1·554	1·348	1·006	1·080	1·089	1·122	1·140	1·069	
6	617·75	419·98	166·72	511·28	377·06	143·02	505·87	370·11	140·54	V95
	473·1	344·2	126·3	473·1	344·2	126·3	473·1	344·2	126·3	VPTV
CI	1·306	1·220	1·320	1·081	1·095	1·132	1·069	1·075	1·113	
7	397·69	349·03	218·99	503·02	360·11	217·97	444·2	352·28	219·58	V95
	416·3	327·1	297·9	416·3	327·1	297·9	416·3	327·1	297·9	VPTV
CI	0·955	1·067	0·735	1·208	1·101	0·732	1·067	1·077	0·737	
8	718·56	437·19	106·41	610·75	444·39	75·48	592·67	459·46	74·14	V95
	555	420·6	66·9	555	420·6	66·9	555	420·6	66·9	VPTV
CI	1·295	1·039	1·591	1·100	1·057	1·128	1·068	1·092	1·108	
9	455·12	358·81	263·55	441·58	325·44	111·2	459·96	368·73	105·19	V95
	417·7	307·7	107·7	417·7	307·7	107·7	417·7	307·7	107·7	VPTV
CI	1·090	1·166	2·447	1·057	1·058	1·032	1·101	1·198	0·977	
10	712·41	532·64	397	633·08	511·64	166·53	629·56	504·73	170·16	V95
	598·8	471·9	165·8	598·8	471·9	165·8	598·8	471·9	165·8	VPTV
CI	1·190	1·129	2·394	1·057	1·084	1·004	1·051	1·070	1·026	

Note: F1, F2, F3 – the three phases of the treatment; CI – the conformity index for each of the ten patients; 3D, IMRT, VMAT the irradiation techniques used and the volumes V95, VPTV in cm^3, see text.

https://doi.org/10.1017/S1460396916000601 Published online by Cambridge University Press

the volume of the PTV (V_{PTV}) (see Equation (1)). A value of CI approaching 1 is more conformal (see Table 2).

$$CI = \frac{V95}{V_{PTV}} \quad (1)$$

The homogeneity index (HI) was likewise computed and is the difference between the near-maximum and near-minimum dose, D2 (D2%) and D98 (D98%), respectively, normalised to the median dose, D50 (D50%) (see Equation (2)) and measures the dose homogeneity over the PTV. A HI value closer to zero shows a more homogenous dose distribution inside the target volume (results, in Table 3).

$$HI = \frac{D_{2\%} - D_{92\%}}{D_{50\%}} \quad (2)$$

Table 3. *Homogeneity index (HI) three-dimensional conformal radiotherapy/intensity modulated radiation therapy/volumetric modulated arc therapy (3D-CRT/IMRT/VMAT)*

	3D			IMRT			VMAT			
	F1	F2	F3	F1	F2	F3	F1	F2	F3	
1	34·66	13·9	3·5	45·39	14·71	3·77	42·22	14·36	3·77	D98
	53·35	17·09	4·26	51·99	16·51	4·08	52·89	16·65	4·13	D2
	50·1	15·92	4	50·36	16·12	4·02	50·62	16·14	4·01	D50
HI	0·373	0·200	0·190	0·131	0·112	0·077	0·211	0·142	0·090	
2	43·28	14·92	3·78	46·67	14·47	3·79	46·77	15·05	3·74	D98
	53·39	17·22	4·07	51·69	16·74	4·08	51·84	16·59	4·15	D2
	50·49	16·48	3·99	50·27	16·12	4·01	50·18	16·04	4·01	D50
HI	0·200	0·140	0·073	0·100	0·141	0·072	0·101	0·096	0·102	
3	45·66	14·58	3·83	47·78	15·31	3·84	46·79	15·29	3·82	D98
	53·33	16·89	4·15	51·6	16·4	4·1	52·05	16·46	4·11	D2
	50·47	15·9	4·06	50·07	16·05	4	50·14	16·03	4	D50
HI	0·152	0·145	0·079	0·076	0·068	0·065	0·105	0·073	0·073	
4	38·98	13·65	3·87	46·73	14·59	3·8	46·03	14·95	3·83	D98
	53·66	17·95	4·19	51·77	16·65	4·06	52·2	16·62	4·14	D2
	50·48	16·39	4·03	50·26	16·11	4·02	50·2	16·06	4	D50
HI	0·291	0·262	0·079	0·100	0·128	0·065	0·123	0·104	0·077	
5	46·13	14·69	3·71	45·08	14·92	3·81	47·05	15·25	3·81	D98
	54·35	17·29	4·1	52·53	16·66	4·07	51·75	16·45	4·12	D2
	50·88	15·9	3·95	50·36	16·05	4·02	50·17	16·04	4	D50
HI	0·162	0·164	0·099	0·148	0·108	0·065	0·094	0·075	0·078	
6	39·97	8·28	5·71	43·8	8·95	4·19	43·44	8·65	3·7	D98
	52·98	10·58	6·07	51·62	10·27	6·17	52·13	10·4	6·31	D2
	50·29	10·02	5·93	50·25	10·08	6·11	50·42	10·09	6·1	D50
HI	0·259	0·230	0·061	0·156	0·131	0·324	0·172	0·173	0·428	
7	36·38	13·14	3·4	47·06	15·05	3·77	46·69	15·16	3·8	D98
	52·43	17·14	4·22	51·57	16·52	4·14	52·22	16·62	4·15	D2
	48·65	15·89	4	50·25	16·06	4·01	50·19	16·04	4	D50
HI	0·330	0·252	0·205	0·090	0·092	0·092	0·110	0·091	0·088	
8	42·54	5·31	3·81	46·89	14·79	3·82	46·76	15·13	3·8	D98
	54·93	16·79	4·24	51·65	16·63	4·07	51·99	16·52	4·12	D2
	49·6	15·54	4·1	50·28	16·1	4·02	50·19	16·05	4·01	D50
HI	0·250	0·739	0·105	0·095	0·114	0·062	0·104	0·087	0·080	
9	42·96	12·05	5·57	42·4	11·34	5·03	39·63	2·19	5·39	D98
	53·48	14·77	6·13	52·02	14·56	6·2	52·2	15·02	6·29	D2
	49·45	13·9	5·96	50·52	14·17	6·1	50·57	14·6	6·06	D50
HI	0·213	0·196	0·094	0·190	0·227	0·192	0·249	0·879	0·149	
10	40·28	13·87	3·65	45·8	14·7	3·17	43·75	14·23	3·69	D98
	54·28	16·93	4·1	52·07	16·54	4·18	52·9	16·78	4·15	D2
	49·53	15·77	3·98	50·34	16·12	4·08	50·52	16·14	4·02	D50
HI	0·283	0·194	0·113	0·125	0·114	0·248	0·181	0·158	0·114	

Note: F1, F2, F3 – the three phases of the treatment; HI – the conformity index for each of the ten patients; 3D, IMRT, VMAT the irradiation techniques used and the values D98, D2, D50 in Gy, see text.

https://doi.org/10.1017/S1460396916000601 Published online by Cambridge University Press

The dose was normalised to a particular percentage to give 95% of the dose to 99% of the PTV. Once each plan was normalised to ensure the PTV dose reflected the prescribed dose, the dose-volume histogram (DVH) data was exported as a .CSV file with a resolution of 0·05 Gy via the export functions embedded in Eclipse for importing into the NTCP calculation software.

As the definition of CI does not consider the positioning and the profile of the 95% isodose volume (V95) in respect to the PTV, we furthermore calculate the Paddick's index which considers the coverage of PTV volume with the 95% isodose. The Paddick's definition of CI is defined as in,[27]

$$\text{Paddick index} = \frac{\text{TV95} \times \text{TV95}}{\text{V95} \times \text{TV}} \qquad (3)$$

where TV95 denotes the target volume inside the 95% isodose volume (V95) (see Table 4).

Table 4. *Paddik's index (PI) three-dimensional conformal radiotherapy/intensity modulated radiation therapy/volumetric modulated arc therapy (3D-CRT/IMRT/VMAT)*

	3D			IMRT			VMAT			
	F1	F2	F3	F1	F2	F3	F1	F2	F3	
1	467·32	290·72	224·4	520·16	339·57	249·82	485·9	326·34	248·69	TV95
	723·71	402·41	282·85	635·87	451·47	270·32	582·82	377·73	267	V95
	555·7	356·1	258·6	555·7	356·1	258·6	555·7	356·1	258·6	VPTV
PI	0·543	0·590	0·688	0·766	0·717	0·893	0·729	0·792	0·896	
2	396·98	269·01	114·24	422·48	254·4	114·52	426·89	268·75	112·74	TV95
	832·18	551	170·82	500·88	295·99	126·55	556·64	343·19	125·88	V95
	448·2	280·2	117·9	448·2	280·2	117·9	448·2	280·2	117·9	VPTV
PI	0·423	0·469	0·648	0·795	0·780	0·879	0·730	0·751	0·856	
3	501·11	343·83	130·71	537·78	367·72	130·7	515·62	366·31	130·17	TV95
	935·58	642·21	194·85	740·88	501·46	157·4	576·22	435	143·53	V95
	547·7	374·3	132·4	547·7	374·3	132·4	547·7	374·3	132·4	VPTV
PI	0·490	0·492	0·662	0·713	0·720	0·820	0·842	0·824	0·892	
4	404·93	308·12	164·42	442·49	319·01	161·07	438·04	329·42	162·63	TV95
	725·98	494·49	250·1	518·86	373·25	184·42	514·87	377·35	181·57	V95
	464·9	344·9	165·3	464·9	344·9	165·3	464·9	344·9	165·3	VPTV
PI	0·486	0·557	0·654	0·812	0·791	0·851	0·802	0·834	0·881	
5	353·72	217·01	78·11	335·41	225·27	81·44	361·67	232·24	81·44	TV95
	631·2	369·63	111·88	379·37	256·81	90·39	423·09	271·02	88·72	V95
	377·2	237·8	83	377·2	237·8	83	377·2	237·8	83	VPTV
PI	0·526	0·536	0·657	0·786	0·831	0·884	0·820	0·837	0·901	
6	406·84	303·33	123·39	442·76	326·31	119·97	436·97	322·53	120·47	TV95
	617·75	419·98	166·72	511·28	377·06	143·02	505·87	370·11	140·54	V95
	473·1	344·2	126·3	473·1	344·2	126·3	473·1	344·2	126·3	VPTV
PI	0·566	0·636	0·723	0·810	0·820	0·797	0·798	0·817	0·818	
7	286·32	256·07	160·95	316·89	314·45	200·09	395·54	316·52	202·75	TV95
	397·69	349·03	218·99	503·02	360·11	217·97	444·2	352·28	219·58	V95
	416·3	327·1	297·9	416·3	327·1	297·9	416·3	327·1	297·9	VPTV
PI	0·495	0·574	0·397	0·480	0·839	0·617	0·846	0·869	0·628	
8	458·15	287·68	65·78	528·97	391·81	65·46	528·98	404·9	65·45	TV95
	718·56	437·19	106·41	610·75	444·39	75·48	592·67	459·46	74·14	V95
	555	420·6	66·9	555	420·6	66·9	555	420·6	66·9	VPTV
PI	0·526	0·450	0·608	0·825	0·821	0·849	0·851	0·848	0·864	
9	332·48	242·59	98·95	387·11	282·94	94·83	386·52	286·31	93·74	TV95
	455·12	358·81	263·55	441·58	325·44	111·2	459·96	368·73	105·19	V95
	417·7	307·7	107·7	417·7	307·7	107·7	417·7	307·7	107·7	VPTV
PI	0·581	0·533	0·345	0·812	0·799	0·751	0·778	0·722	0·776	
10	477·44	372·92	151·74	556·97	444·18	144·99	517·56	426·37	155·6	TV95
	712·41	532·64	397	633·08	511·64	166·53	629·56	504·73	170·16	V95
	598·8	471·9	165·8	598·8	471·9	165·8	598·8	471·9	165·8	VPTV
PI	0·534	0·553	0·350	0·818	0·817	0·761	0·711	0·763	0·858	

Note: F1, F2, F3 – the three phases of the treatment; PI – the Paddick's index for each of the 10 patients; 3D, IMRT, VMAT the irradiation techniques used and the values TV95, V95, VPTV in cm^3, like defined in text.

https://doi.org/10.1017/S1460396916000601 Published online by Cambridge University Press

Radiobiology models

NTCP were ascertained utilising the EUD scientific models and programming code portrayed by Gay and Niemierko.[28] Gay and Niemierko models determine EUD from the DVH and apply a parameter 'a' which is particular to either a tumour or an organ at risk. The parameter 'a' can drive the EUD to denote maximal, minimal or mean dose. On account of tumours, 'a' parameter is a big negative number, so that the EUD for tumours is near the minimal dose. For normal tissues with serial like organisation, 'a' parameter will be a large positive number. For normal tissues that present an extensive volume impact, 'a' will be a small positive number.

Values for the 'a' parameter utilised in NTCP calculation are displayed in Table 5 and were picked from the references listed in this table, or from the values suggested by Gay and Niemierko.[28] The NTCP models likewise require values for the α/β ratio, TD50 (the dose for half complication rate probability) for normal tissues and $\gamma 50$ (slope of the dose response curve).

Another NTCP calculating model was Lyman–Kutcher–Burman (LKB)[29,30] with DVH parameterised as the EUD,[31] given by the equations below:

$$\mathrm{NTCP} = \frac{1}{\sqrt{2\pi}} \int_{-\infty}^{t} \exp\left(-x^2/2\right) dx \qquad (4)$$

$$t = \left(\mathrm{EUD} - \mathrm{TD}_{50}\right)/_{m} \cdot \mathrm{TD}_{50} \qquad (5)$$

$$\mathrm{EUD} = \left(\sum_i v_i D_i^{\frac{1}{n}}\right)^n \qquad (6)$$

The DVH is conformed to the EUD through a power-law relationship. v_i is the volume of the dose bin corresponding to dose D_i in the differential DVH. n depicts the volume correlation with the organ where: $n = 0$ shows a totally serial structure and $n = 1$ demonstrates a parallel structure. m is the slope steepness of the dose response curve and TD50 is the dose which can lead to a 50% complication probability when delivered to the entire organ.

RESULTS AND DISCUSSION

Dosimetric result

Dosimetric result Figure 2 demonstrates the dosimetric results of the plans made utilising 3D-CRT, IMRT or VMAT methods.

Target volume CI, HI and Paddick's index

The mean CI for 3D-CRT was ($1{\cdot}424 \pm 0{\cdot}013$), for IMRT ($1{\cdot}100 \pm 0{\cdot}004$) and for VMAT ($1{\cdot}081 \pm 0{\cdot}003$). The HI index was ($0{\cdot}204 \pm 0{\cdot}004$) for 3D-CRT, ($0{\cdot}124 \pm 0{\cdot}002$) for IMRT and ($0{\cdot}153 \pm 0{\cdot}005$) for VMAT. The Paddick index was smaller for 3D-CRT than IMRT ($-0{\cdot}246$, $p < 0{\cdot}001$), and VMAT ($-0{\cdot}268$, $p < 0{\cdot}001$). The Paddick index difference between IMRT and VMAT ($0{\cdot}022$, $p < 0{\cdot}015$) was found clinically insignificant (Tables 2–4).

Table 5. *Values for the parameters used in the normal tissue complication probability calculations*

	Gay and Niemierko						
	fx	**α/β**	**Dose/fx**	**a**	**γ(50%)**	**TD 50%**	**Reference**
Brain	35	2·9	2	5	3	60	24
Brainstem	35	2·5	2	7	3	65	24
Optic chiasm	35	2	2	25	3	65	24
Spinal cord	35	2	2	13	2	66·5	24
Optic nerve	35	1·6	2	25	3	55	24
	LKB						
	fx	**α/β**	***n***	**m**	**TD 50%**	**Reference**	
Brain	35	2·9	0·25	0·15	60	24	
Brainstem	35	2·5	0·16	0·14	65	24	
Optic chiasm	35	2	0·25	0·14	65	24	
Optic nerve	35	1·6	0·25	0·14	65	24	
Spinal cord	35	2	0·05	0·175	66·5	24	

LKB, Lyman–Kutcher–Burman.

https://doi.org/10.1017/S1460396916000601 Published online by Cambridge University Press

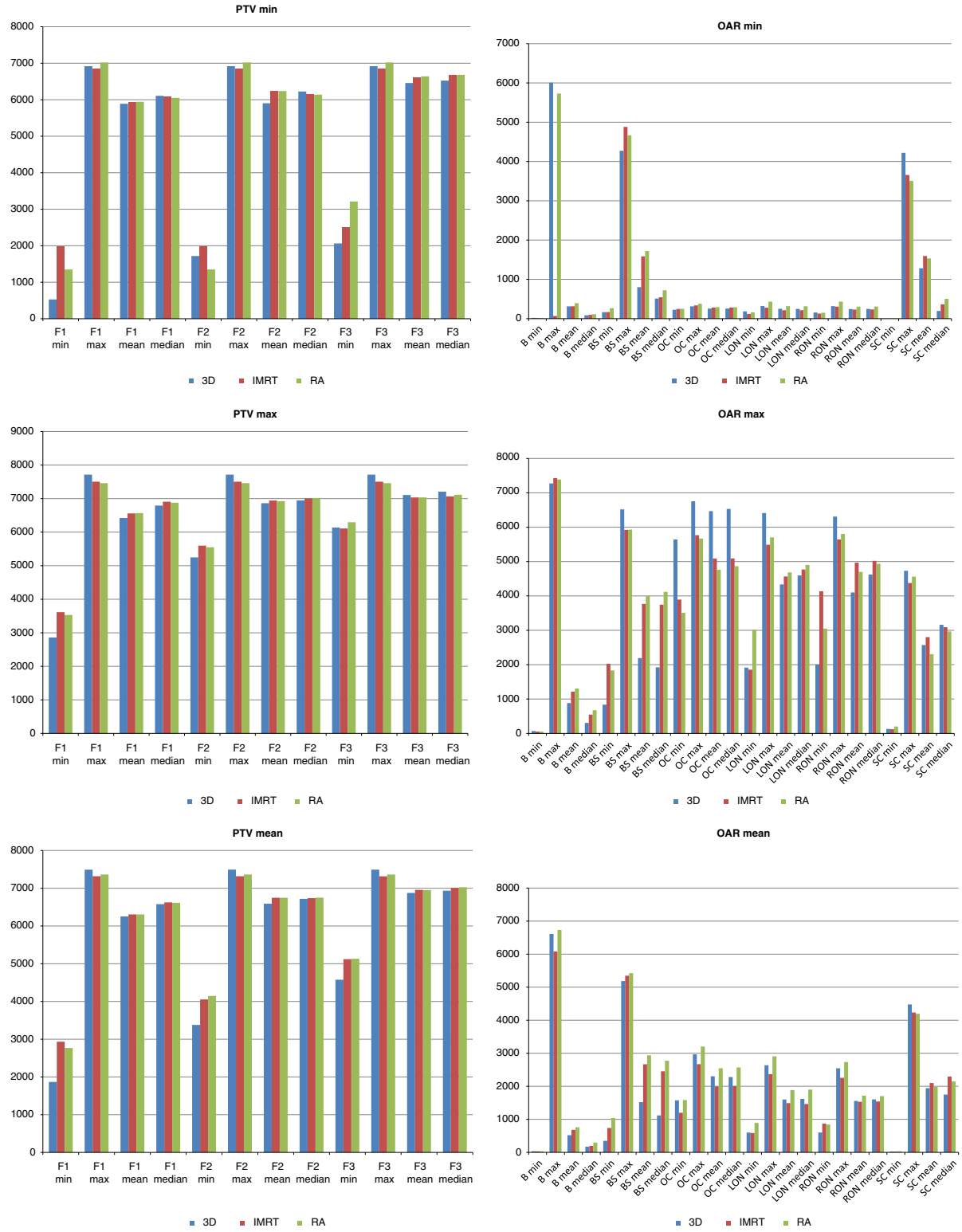

Figure 2. Dosimetric values for three stages nasopharyngeal cancer treatment (dose in cGy). Abbreviations: PTV, planning target volume; OAR, organ at risk.

https://doi.org/10.1017/S1460396916000601 Published online by Cambridge University Press

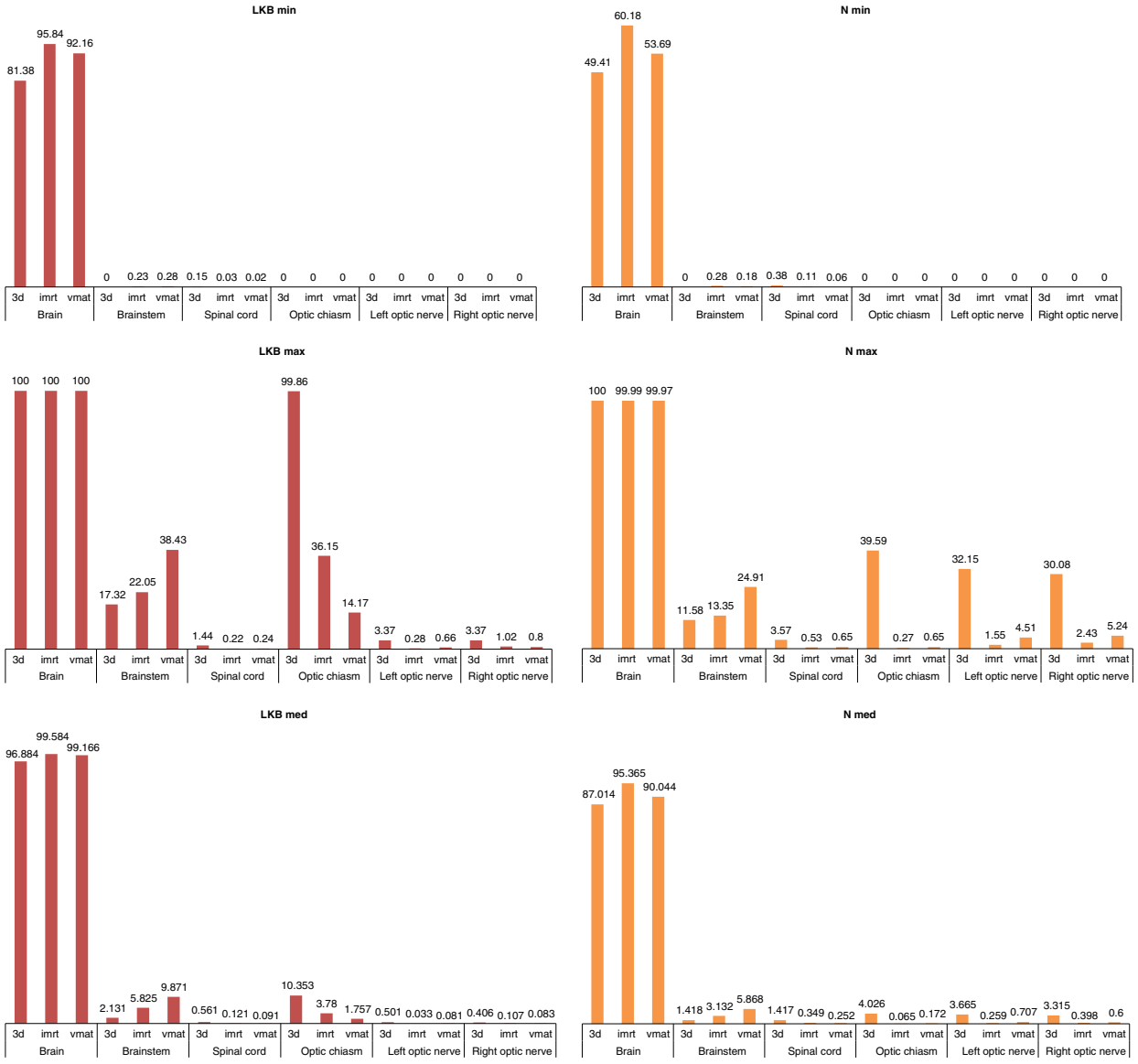

Figure 3. Normal tissue complication probabilities (values in %). Abbreviation: LKB, Lyman–Kutcher–Burman.

MUs

The mean MUs was least for 3D-CRT at 95 (range 9–180); was 165 (range 52–277) for IMRT, and highest at 331 (range 167–494) for VMAT ($p < 0{\cdot}05$).

Normal tissue complication probabilities

Figure 3 shows the NTCP distribution for 3D-CRT, IMRT and VMAT. We used RADBIOMOD, a simple program for calculation of complication probabilities.[24]

DISCUSSION

This study parallels VMAT with dynamic MLC, IMRT and 3D-CRT for 10 patients with nasopharyngeal cancer. The main concern in the treatment of head-and-neck cases is the concave shape of the tumour and the closeness of normal structures to the tumour. IMRT has been the typical treatment technique for head-and-neck cancer.

Acute and late toxicity was the most important problem during the time of conventional

https://doi.org/10.1017/S1460396916000601 Published online by Cambridge University Press

radiotherapy. Replacing cobalt machines with linear accelerators made possible dose escalation using high energy photons whose dosimetric profile has allowed the treatment of deep tumours, at the same time limiting the skin dose. IMRT and VMAT techniques implementation offered the advantage of optimising delivery of the radiation dose in the target volume with irregular shapes and superior protection of organs at risk. IMRT has enabled the delivery of different doses and fractions using integrated boost techniques or by selecting some through 'dose painting' escalating dose in the macroscopic disease and irradiating with a reduced dose in areas suspected of microscopic dissemination.[32,33]

Combined treatment with platinum-based chemotherapy or monoclonal anti-bodies, modified the radiotherapy toxicity profile and improved local control. The desire to improve the quality of life of patients with head-and-neck cancers led to the need of reducing the adverse effects like xerostomia and reducing the dose to the parotid glands under 26 Gy. Using dose constriction validated after studies of over 25 years of 2D and 3D radiotherapy on classic fractionation schemes (2 Gy/fraction) may be too tolerant in light of new techniques. Many of the patients treated according to new therapeutic standards will be long time survivors and requires validation of new models of late toxicity. Lee et al. reported, for the initial batch of nasopharyngeal cancer patients initially treated with IMRT technique, a local control rate of 97% after four years although 70% of patients had locally advanced disease.[33–36]

Radiation Therapy Oncology Group 0225 trial [37] demonstrated the feasibility of IMRT technique implementation as standard in nasopharyngeal cancer treatment, this phase II trial achieving 93% local control, 89% loco regional control and 80% overall survival.[36] One cannot ignore the benefit of positron emission tomography–computed tomography (PET-CT) and magnetic resonance imaging (MRI) techniques used in diagnosis which have improved remote extension evaluation (PET-CT) and the skull base invasion where MRI imaging has proved its superiority. All these factors have led to improved prognosis and the need to focus attention on possible late toxicities. In the era of conventional radiotherapy, limiting the dose to the spinal cord was the main concern for oncologists as radiation-induced severe myelitis was a known late effect of irradiation. The late effects of irradiation on brain tissue with high doses have been neglected. Radionecrosis of temporal lobe and hippocampus irradiation lead to deterioration in cognitive function with consequences on the quality of life by the occurrence of radio-induced dementia or even death.[38,39] Complex profiles of DVH curves and the decrease of volumes receiving high-dose compared with volumes irradiated with low dose made it difficult to assess and evaluate plans obtained through IMRT and VMAT techniques. Implementation of mathematical-radiobiological models became necessary in order to give the patient the best possible plan, optimised for clinical and prognostic features, allowing one to obtain optimal balance between achieving local control and reducing toxicity which can affect the quality of life or in extreme cases can be fatal.[32,34]

D_{min} received by target volumes is comparable for all three methods in all treatment phases. In some cases for phase I and III 'cold spots' may occur by using 3D-CRT method while risk of under dosage in phase II is higher for VMAT plans. D_{mean} and D_{max} again are comparable for all methods but conformity, uniformity and Paddick, could be the best indicators for dosimetric coverage of target volumes. D_{min} for aperture optics (optic nerves, optic chiasm, eyes) are similar in value.

For brain, using 3D-CRT and VMAT techniques produced considerably higher doses than using the IMRT technique, in some cases, but considerably higher doses than through IMRT method were obtained, in some cases but average doses for all patients were within normal limits. For brainstem inverse planning techniques obtained average and maximum values of D_{min} higher than 3D-CRT method. D_{max} higher values (sometimes over 70 Gy) for brain obtained in some patients for all three techniques, significantly increased the risk of cerebral radionecrosis. High values of D_{max} for optical aperture were received using the 3D

https://doi.org/10.1017/S1460396916000601 Published online by Cambridge University Press

technique and therefore justify the implementation of IMRT and VMAT techniques as standard radiotherapy methods for nasopharynx tumours treatment.[34]

Increased D_{mean} by using VMAT for brain, brainstem and optical aperture is not a drawback if associated with the decrease of hotspots and with smaller volumes receiving high doses, thereby reducing the risk of radionecrosis and fibrosis. Maintaining maximum dose received within existing dosimetric guidelines is a safe solution for limiting the aperture optics toxicity $D < 50$ Gy, $D_{max} = 54$ Gy (with a risk of optic neuropathy <3%), $D_{max} = 55$–60 Gy (risk estimated between 3 and 7%) and $D_{max} = 60$ Gy (risk of toxicity up to 20%).

Serial architecture of the spinal cord from the point of view of radiobiological effects, is a risk factor for radio-induced myelitis even if small portions of this organ are irradiated with high doses. The effect of 'bath and shower' which means the presence of high dose close to low-dose regions, which is characteristic for inverse planning dosimetry, increases the risk of bone marrow toxicity. The risk of Lhermitte's syndrome occurs among patients treated with IMRT and the advantages and limits of modern techniques are difficult to evaluate in the absence of clinical trials for extended periods of time.[32]

Evaluation of treatment plans using radiobiological models with the aim of reducing cerebral necrosis assists the multidisciplinary team involved in therapeutic decision to choose the best solutions that maintain benefit – toxicity balance. Gay and Niemierko's model is more permissive in predicting risk of brain tissue radionecrosis while LKB model predicts a 50–60% risk, indicating that at least one patient in the study group will develop brain toxicity as a late complication. For both models the maximum risk of radionecrosis is estimated to be over 90%. VMAT technique significantly increases the risk of brainstem radionecrosis if we are not performing optimisation of treatment plans to reduce the doses received by the brain, the LKB model predicting a greater risk than Gay and Niemierko's one.[28,33,35]

Both inverse planning techniques estimated radionecrosis risk of brainstem higher than 3D-CRT plans. Considering the gravity of this complication, it is necessary to reduce $V < 1$–$10\ cm^3$ <59 Gy and $V < 1\ cm^3$ <64 Gy. The optic chiasm toxicity risk is about five times higher for the 3D-CRT technique with averages of about 10–4% predicted by LKB model and Niemierko model, respectively.[33,34]

The Gay and Niemierko model estimates an ~3% and a maximum of 30% risk of necrosis to the optic nerves using 3D-CRT technique and subunit values of risk when using IMRT and VMAT techniques. Dunlop et al. have proposed a way to avoid brain irradiation when treating nasopharyngeal cancer. This is by generating IMRT non-coplanar plans and delineating and imposing dosimetric constraints for the structures involved in cognitive function defined as organ at risk, then NTCP values were calculated. With the aim of reducing the risk to neurocognitive function, a significant reduction in 80% of plans and a significant dose reduction for hippocampus, brain and brainstem.[34]

Jing Cheena et al. appreciate the need of a careful evaluation of brain radionecrosis using complex imagery techniques (18-FDG-PET, MRI spectroscopy, single-photon emission computed tomography) and identify risk factors for base of skull and cavernous sinus invasion. Temporal lobe radiation-induced necrosis estimated risk is 4·6% at 10 years for $D > 60$ Gy using standard fractionation increasing to 35% at 3·5 years using accelerated fractionation. A study by Kam proves that IMRT can reduce D_{max} for the temporal lobe to 46 Gy compared with 66·5 Gy received using 2D technique in a case of a locally advanced T4N2M0 nasopharynx cancer. Re-planning after 25 fractions can also significantly reduce the dose received by the temporal lobe. The risk of cerebral necrosis is considered 0% for a dose of 66 Gy given in 33 fractions and 14% for a dose of 72 Gy/40 fractions/35 days.[34,36,40–42]

Yeh et al. consider that a 72 Gy dose in standard fractionation scheme is associated with a high risk of cerebral toxicity. If a 7–15 Gy stereotactic boost is added to a dose of 66 Gy the risk increases to 12%. Su considered that the

https://doi.org/10.1017/S1460396916000601 Published online by Cambridge University Press

incidence of temporal lobe injury is relatively high, especially for patients with advanced T-stage, and correlated with D_{max} and D 1 cm^3 and for IMRT $D_{max} < 68$ Gy D 1 cm^3 <58 Gy is relatively safe. Also clinical comorbidities like diabetes, hypertension, dyslipidemia and obesity decreases brain tissue tolerance to radiation and the treatment with anticoagulant drugs, corticosteroids, hyperbaric oxygen and epidermal growth factor receptor inhibitors (Bevacizumab) provide a protective effect and may delay or improve the radionecrosis effect.[34,42–48]

In our study, IMRT and VMAT plans are similar regarding the dose distribution (high conformity, homogeneity and superior Paddick indices relative to 3D-CRT technique). The Paddick index difference between IMRT and VMAT is considered clinically insignificant. IMRT has higher MUs in contrast with 3D-CRT and is liable to increase the integral dose.[49] Ruben et al. consider the risk of a radiation-induced secondary malignancy as small based on the low and middle doses spread by IMRT.[50] While IMRT increases the MUs demand compared with 3D-CRT, the smaller field size and reduced average field intensity have been reported to reduce the scatter more than enough to compensate for any increase in head leakage.[50] Typically, a reduction in MUs required with VMAT diminishes exposure to leaked radiation from the gantry head: a concern in regards to increasing the risk of a radiation-induced malignancy.[51] However, VMAT delivers dose circumferentially around patients, conceivably leading to an expansion in the volume of normal tissue exposed to low radiation doses. However, in our study, we found that MUs with VMAT were fundamentally higher than for IMRT, as both the delivered dose distribution and leakage radiation assume a part in storing dose outside the treatment volume, the potential for secondary malignancies to develop many years after treatment, remains uncertain for long-term survivors receiving these two techniques.[52]

Reduced MUs do have other advantages in the running of radiotherapy departments, including extended linear accelerator lifespan, reduced shielding requirements as well as the likely economic benefit of a faster treatment. In addition, the decrease in treatment times with the utilisation of VMAT is especially valuable for patient comfort and lessening of the contact time between the skin and the thermoplastic mask.

CONCLUSIONS

We were able to demonstrate that IMRT and VMAT plans are similar in terms of dose distributions and both have superior CIs when compared with 3D-CRT. Given the benefits in terms of reduced MUs as well as treatment time, VMAT appears to be the ideal technique to be used with image-guided or adaptive radiotherapy for nasopharyngeal cancer. IMRT and VMAT plans complexity associated with improved survival in nasopharyngeal cancer patients even in advanced forms make necessary a careful consideration for dosimetric predictors of toxicity that can severely impair cognitive function of the brain, potentially decreasing the quality of life for long-term survivors.

Biological models Gay and Niemierko, and LKB offer an easier method for plan benchmarking, but may not substitute the DVH-based evaluations and predictive accuracy must be confirmed by clinical studies. Brain radionecrosis severity and risk were previously underestimated and as the life expectancy of patients with nasopharyngeal cancer is improving, maintaining of neural structures under recommended dose limits should be considered as a first degree priority when IMRT and VMAT plans are implemented.

The discussion in a multidisciplinary team should take into account consideration of the NTCP values and the possible impact these may have on cerebral necrosis and neurocognitive function. This could give the patient the best plan solution in the clinical context, life expectancy and the aim to achieve local control whilst maintaining the balance between effects and toxicities.

Acknowledgment

The authors wish to thank to the anonymous referees who use significant time and effort to provide their expert views, to improve our manuscript.

https://doi.org/10.1017/S1460396916000601 Published online by Cambridge University Press

References

1. Sun Y, Zhou G, Qi Z, Zhang L et al. Radiation-induced temporal lobe injury after intensity modulated radiotherapy in nasopharyngeal carcinoma patients: a dose-volume-outcome analysis. BMC Cancer 2013; 13: 397.
2. Dassarath M, Yin Z, Chen J, Liu H et al. Temporal lobe necrosis: a dwindling entity in a patient with nasopharyngeal cancer after radiation therapy. Head Neck Oncol 2011; 10: 3–8.
3. Gaya A, Mahadevan A. (eds)Stereotactic body radiotherapy. a practical guide. Future Oncol 2014; 10 (15): 2307–2310.
4. Chen J, Dassarath M, Yin Z et al. Radiation induced temporal lobe necrosis in patients with nasopharyngeal carcinoma: a review of new avenues in its management. Radiat Oncol 2011; 30: 6–128.
5. Gocheva L. Radiation tolerance of spinal cord: doctrine, dogmas, data. Archf Oncol 2000; 8 (3): 131–134.
6. Kirkpatrick J P, Van der Kogel A J, Schultheiss T E et al. Radiation dose–volume effects in the spinal cord. Int J Radiat Oncol Biol Phys 2010; 76 (3 suppl): S42–S49.
7. Lim D C, Gagnon P J, Meranvil S, Darryl K, Linda L, John M H. Lhermitte's sign developing after imrt for head and neck cancer. Int J Otolaryngol 2010; 2010: 1–4.
8. Pak D, Vineberg K, Feng F et al. Lhermitte's syndrome after chemo-IMRT of head and neck cancer: incidence, doses, and potential mechanisms. Int J Radiat Oncol Biol Phys 2012; 83 (5): 1528–1533.
9. Mayo C, Yorke E, Merchant T E et al. Radiation associated brainstem injury. Int J Radiat Oncol Biol Phys 2010; 76 (3 suppl): S36–S41.
10. Lee V, Leung T, Kwong D. Dosimetric predictors of radiation-induced acute nausea and vomiting in IMRT for nasopharyngeal cancer. Int J Radiat Oncol Biol Phys 2012; 84 (1): 176–182.
11. Ciura K, McBurney M, Nguyen B et al. Effect of brain stem and dorsal vagus complex dosimetry on nausea and vomiting in head and neck intensity-modulated radiation therapy. Med Dosim 2011; 36 (1): 41–45.
12. Pow E H, Kwong D L, McMillan A S et al. Xerostomia and quality of life after intensity-modulated radiotherapy vs. conventional radiotherapy for early-stage nasopharyngeal carcinoma: Initial report on a randomized controlled clinical trial. Int J Radiat Oncol Biol Phys 2006; 66: 981–991.
13. Braam P M, Terhaard C H, Roesink J M et al. Intensity-modulated radiotherapy significantly reduces xerostomia compared with conventional radiotherapy. Int J Radiat Oncol Biol Phys 2006; 66: 975–980.
14. Dijkema T, Terhaard C H, Roesink J M et al. Large cohort dose volume response analysis of parotid gland function after radiotherapy: Intensity-modulated versus conventional radiotherapy. Int J Radiat Oncol Biol Phys 2008; 72 (4): 1101–1109.
15 Eisbruch A, Ship J A, Dawson L A et al. Salivary gland sparing and improved target irradiation by conformal and intensity modulated irradiation of head and neck cancer. World J Surg 2003; 27: 832–837.
16. Chui C S, Chan M F, Spirou S et al. Delivery of intensity-modulated radiation therapy with a conventional multileaf collimator: comparison of dynamic and segmental methods. Med Phys 2001; 28: 2441–2449.
17. Pirzkall A, Carol M P, Pickett B et al. The effect of beam energy and number of fields on photon-based IMRT for deep-seated targets. Int J Radiat Oncol Biol Phys 2002; 53: 434–442.
18. Cameron C. Sweeping-window arc therapy: and implementation of rotational IMRT with automatic beam-weight calculation. Phys Med Biol 2005; 50: 4317–4336.
19. Earl M A, Shepard D M, Naqvi S et al. Inverse planning for intensity-modulated arc therapy using direct aperture optimization. Phys Med Biol 2003; 48: 1075–1089.
20. Yu C X, Li X A, Ma L et al. Clinical implementation of intensity-modulated arc therapy. Int J Radiat Oncol Biol Phys 2002; 53: 453–463.
21. Otto K. Volumetric modulated arc therapy: IMRT in a single gantry arc. Med Phys 2008; 35: 310–317.
22. Das I J, Cheng C W, Chopra K L et al. Intensity-modulated radiation therapy dose prescription, recording, and delivery: patterns of variability among institutions and treatment planning systems. J Natl Cancer Inst 2008; 100: 300–307.
23. Galvin J M, Ezzell G, Eisbrauch A et al. Implementing IMRT in clinical practice: a joint document of the American Society for Therapeutic Radiology and Oncology and the American Association of Physicists in Medicine. Int J Radiat Oncol Biol Phys 2004; 58 (5): 1616–1634.
24. Chang J H, Gehrke C, Prabhakar R et al. RADBIOMOD: a simple program for utilising biological modelling in radiotherapy plan evaluation. Physica Medica 2016; 32: 248–254.
25. Van Gestel D, Van Den Weyngaert D, Schrijvers D. Intensity-modulated radiotherapy in patients with head and neck cancer: a European single-centre experience. Br J Radiol 2011; 84 (1000): 367–374.
26. Dobbs J E, Barrett A, Roques T. Practical Radiotherapy Planning, 4th edition. Boca Raton, FL: CRC Press, 2009.
27. Paddick I. A simple scoring ratio to index the conformity of radiosurgical treatment plans. Technical note. J Neurosurg 2000; 93 (suppl 3): 219–222.
28. Gay H A, Niemierko A. A free program for calculating EUD-based NTCP and TCP in external beam radiotherapy. Phys Med 2007; 23: 115–125.

https://doi.org/10.1017/S1460396916000601 Published online by Cambridge University Press

29. Lyman J T. Complication probability as assessed from dose-volume histograms. Radiat Res 1985 1985; 104: S13–S19.

30. Burman C, Kutcher G J, Emami B, Goitein M. Fitting of normal tissue tolerance data to an analytic function. Int J Radiat Oncol Biol Phys 1991; 21: 123–135.

31. Niemierko A. A generalized concept of equivalent uniform dose (EUD). Med Phys 1999; 26: 1100.

32. Nishimura Y, Komaki R. Intensity-Modulated Radiation Therapy, Clinical Evidence and Techniques. Tokio: Springer, 2015.

33. van der Kogel A, Joiner M. Basic Clinical Radiobiology, 4th edition. London: Hodder Arnold Publication, 2009.

34. Dunlop A, Welsh L, McQuaid D. Brain-sparing methods for IMRT of head and neck cancer. PLoS One 2015; 10 (3): e0120141.

35. Rubin P, Constine L S, Marks L B. ALERT Adverse Late Effects of Cancer Treatment: Volume 1: General Concepts and Specific Precepts, Volume 2: Normal Tissue Specific Sites and Systems. New York: Springer, 2014.

36. Lee A W, Tung S Y, Chan A T et al. Preliminary results of a randomized study (NPC-9902 Trial) on therapeutic gain by concurrent chemotherapy and/or accelerated fractionation for locally advanced nasopharyngeal carcinoma. Int J Radiat Oncol Biol Phys 2006; 66: 142–151.

37. Lee N, Harris J, Garden A S, Straube W, Glisson B et al Intensity-modulated radiation therapy with or without chemotherapy for nasopharyngeal carcinoma: radiation therapy oncology group phase II trial 0225, J Clin Oncol 2009; 27 (22): 3684–3690.

38. Wu X, Gu M, Zhou G et al. Cognitive and neuropsychiatric impairment in cerebral radionecrosis patients after radiotherapy of nasopharyngeal carcinoma. BMC Neurol 2014; 14: 10.

39. Cheung M, Chan A S, Law S C et al. Cognitive function of patients with nasopharyngeal carcinoma with and without temporal lobe radionecrosis. Arch Neurol 2000; 57 (9): 1347–1352.

40. Kam M K M, Teo P M L, Chau R M C et al. Treatment of nasopharyngeal carcinoma with intensity-modulated radiotherapy: the Hong Kong experience. Int J Radiat Oncol Biol Phys 2004; 60: 1440–1450.

41. Zeng L, Tian Y M, Sun X M et al. Late toxicities after intensity-modulated radiotherapy for nasopharyngeal carcinoma: patient and treatment-related risk factors. Br J Cancer 2014; 110: 49–54.

42. Yeh S A, Tang Y, Lui C C, Huang Y J, Huang E Y et al. Treatment outcomes and late complications of 849 patients with nasopharyngeal carcinoma treated with radiotherapy alone. Int J Radiat Oncol Biol Phys 2005; 62: 672–679.

43. Lee A W, Ng W T, Chan L L et al. Evolution of treatment for nasopharyngeal cancer – success and setback in the intensity-modulated radiotherapy era. Radiother Oncol 2014; 110: 377–384.

44. Lee P W, Hung B K, Woo E K, Tai P T, Choi D T. Effects of radiation therapy on neuropsychological functioning in patients with nasopharyngeal carcinoma. J Neurol Neurosurg Psychiatr 1989; 52: 488–492.

45. Takiar V, Ma D, Garden A S et al. Disease control and toxicity outcomes for T4 carcinoma of the nasopharynx treated with intensity-modulated radiotherapy. Head Neck 2016; 38 (suppl 1): E925–E933.

46. Zheng Y, Han F, Xiao W et al. Analysis of late toxicity in nasopharyngeal carcinoma patients treated with intensity modulated radiation therapy. Radiat Oncol 2015; 13: 10–17.

47. Bortfeld T, Schmidt-Ullrich R, De Neve W, Wazer D E. Image-Guided IMRT. Berlin, Heidelberg: Springer, 2016.

48. Su S F, Huang Y, Xiao W W et al. Clinical and dosimetric characteristics of temporal lobe injury following intensity modulated radiotherapy of nasopharyngeal carcinoma. Radiother Oncol 2012; 104 (3): 312–316.

49. Hall E J, Wuu C S. Radiation-induced second cancers: the impact of 3D-CRT and IMRT. Int J Radiat Oncol Biol Phys 2003; 56: 83–88.

50. Ruben J D, Davis S, Evans C et al. The effect of intensity-modulated radiotherapy on radiation-induced second malignancies. Int J Radiat Oncol Biol Phys 2008; 70: 1530–1536.

51. Hall E J. Intensity-modulated radiation therapy, protons, and the risk of second cancers. Int J Radiat Oncol Biol Phys 2006; 65: 1–7.

52. Davidson M T, Blake S J, Batchelar D L, Cheung P, Mah K. Assessing the role of volumetric modulated arc therapy (VMAT) relative to IMRT and helical tomotherapy in the management of localized, locally advanced, and post-operative prostate cancer. Int J Radiat Oncol Biol Phys 2011; 80: 1550–1558.

https://doi.org/10.1017/S1460396916000601 Published online by Cambridge University Press